Nonlocal permittivity from a quasistatic model for a class of wire media

Stanislav I. Maslovski[*] and Mário G. Silveirinha

Departamento de Engenharia Electrotécnica, Instituto de Telecomunicações, Universidade de Coimbra–Pólo II,
3030-290 Coimbra, Portugal

A simple quasistatic model applicable to a wide class of wire media is developed that explains strong nonlocality in the dielectric response of wire media in the very long wavelength limit in clear physical terms of effective inductance and capacitance per unit length of a wire. The model is checked against known solutions and found to be in excellent agreement with the results obtained by much more sophisticated analytical and numerical methods. Special attention is given to suppression of the spatial dispersion effects in wire media.

I. INTRODUCTION

Wire media are structured materials formed by many conducting wires embedded in a host medium. The wires are normally considered to be very long compared to the wavelength in the host medium, but the diameter of the wires is only a small fraction of the lattice constant. The known analytical models of wire media[1–13] treat them as crystals of infinitely long conducting cylinders. The cylinders may be arranged in different types of lattices resulting in different types of anisotropy of the wire crystals. It is known that wire media may exhibit strong spatial dispersion at wavelengths orders of magnitude larger than the characteristic size of the unit cell, so that the permittivity dyadic $\bar{\bar{\varepsilon}}(\omega,\mathbf{k})$ in such media depends on both frequency and wave vector even in the very long wavelength limit.[9] For instance, the permittivity dyadic of uniaxial wire medium with one set of thin ideally conducting wires oriented along $\mathbf{z}_0$ reads[9]

$$\frac{\bar{\bar{\varepsilon}}(\omega,\mathbf{k})}{\varepsilon_0} = \bar{\bar{I}}_t + \left(1 - \frac{k_p^2}{k_0^2 - k_z^2}\right)\mathbf{z}_0\mathbf{z}_0, \qquad (1)$$

where $k_0 = \omega\sqrt{\varepsilon_0\mu_0}$, ε_0, and μ_0 are the permittivity and the permeability of the host medium, which is assumed, without any loss of generality, to be vacuum, k_p is the plasma wavenumber, k_z is the wave vector component along $\mathbf{z}_0$, and $\bar{\bar{I}}_t$ is the unit dyadic in the plane orthogonal to $\mathbf{z}_0$.

It is well-known that the wire medium supports propagation of transverse electromagnetic modes (TEM), which are basically the modes of a multiwire transmission line.[9,12] Such modes propagate along the wires with the velocity equal to the speed of light in the host medium. The distribution of the microscopic **E** and **H** fields associated with the TEM modes is staticlike in the planes orthogonal to the wires, with the electric force lines emerging from and ending at the surfaces of the wires. It can be easily proven that there is electrical charge accumulated on the wires associated with these modes. In Ref. 14, it was shown (for the uniaxial wire medium case) that when this charge and the related potential are taken into account it is possible to obtain Eq. (1) from simple quasistatic considerations similar to those used in Ref. 5. Thus, it was shown that the strong spatial dispersion in wire media can be correctly described in a quasistatic approximation. In this paper, we extend these considerations to a wide

class of wire media, and propose an analytical model based on the effective inductance and capacitance per unit length of a wire.

The other motivation for this study is the suppression of the nonlocal effects in wire media. In a recent paper by Demetriadou and Pendry,[15] the charge accumulated on the wires together with the rather small capacitance of thin wires were identified as the reasons for the spatial dispersion in wire mesh: a metamaterial formed by three sets of wires oriented along three Cartesian coordinate axes and joined at the crossing points. A rigorous analytical model of such medium was developed in Refs. 11 and 13. The authors of Ref. 15 make use of this model and full wave simulations to justify their main claims. They also propose certain ways how to decrease the spatial dispersion effects. The basic idea is to increase the capacitance of the wires by periodically loading them with metallic bodies or patches, or alternatively to increase the inductance per unit length by coating the wires with a magnetic material. Somehow related to this work, it was shown in Refs. 16 and 17 that for a substrate formed by a wire medium slab capped with an array of patches (the so-called mushroom substrate)[18] the response of the wire medium is essentially local. A different strategy to reduce the spatial dispersion was reported in Ref. 13, where it was shown that at infrared frequencies the plasmonic properties of metals may enable the design of artificial plasmas that mimic more closely a continuous local isotropic medium with negative permittivity.

In this work, we generalize the theories reported in previous studies, and propose a quasistatic homogenization model that accurately characterizes the nonlocal dielectric function of a wide class of wire media (both arrays of parallel wires, and arrays of connected wires), including the case where the wires are periodically loaded with conducting metallic bodies. In particular, we demonstrate that our analytical theory models accurately the electric response of a uniaxial wire medium loaded with patches, and we discuss the physics of the suppression of spatial dispersion in such structures.

II. UNIAXIAL WIRE MEDIUM

We will start with the simplest possible case of the uniaxial wire medium with one set of wires oriented along
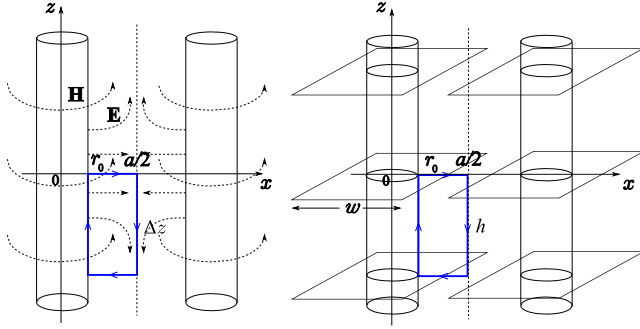
FIG. 1. (Color online) A pair of wires of the uniaxial wire medium without (on the left) and with patches (on the right). The integration path used to define Eq. (4) is shown by the blue rectangular contour marked with arrows.

the z axis. We will follow the treatment presented in Ref. 14.

We are interested in the longitudinal (zz) component of the permittivity dyadic. To get an expression for it in the quasistatic limit, we assume that the radius of the wires r_0 and the distance between the wires (the lattice period) a are much less than the wavelength in the medium. The wires can be arranged in a square lattice or a hexagonal lattice. We will treat both cases with the same model and will show that the difference in the unit cell geometry has insignificant impact when $r_0 \lesssim a/5$.

Denoting the average (macroscopic) electric field along z axis in the medium by $\langle E_z \rangle$, one can write the following relation between this field component and the current in the wires I_z:

$$\langle E_z \rangle = (j\omega L + Z_w)I_z + \frac{\partial \varphi}{\partial z}, \qquad (2)$$

where L is the effective inductance per unit length of the wire, Z_w is the self-impedance of the wire per unit length, which accounts for the finite conductivity of metallic wires at microwave frequencies or plasmonic behavior at optical frequencies, and φ is the additional potential due to charges on the wires.

This relation can be obtained integrating the microscopic electric field over a path shown in Fig. 1. The path goes first along the surface of a wire then to the middle line in a pair of two neighboring wires, then along this middle line and, finally, back to the surface of the wire. The circulation of the microscopic electric field $\mathbf{E}(x,z)$ over this path reads

$$\oint \mathbf{E} \cdot \mathbf{dl} = \int_z^{z+\Delta z} E_z(r_0,z')dz' - \int_z^{z+\Delta z} E_z(a/2,z')dz'$$
$$+ \int_{r_0}^{a/2} E_x(x,z+\Delta z)dx - \int_{r_0}^{a/2} E_x(x,z)dx. \qquad (3)$$

The first integral in this relation represents the voltage drop along the surface of the wire and, therefore, can be expressed in terms of the wire current and the wire self-impedance per unit length. The second integral is the voltage drop along the symmetry line shown in Fig. 1. In the same manner as it was done in Ref. 5, we relate this voltage drop with the macro-

scopic electric field in the medium. After doing this, the circulation of the electric field reads (when Δz is small enough)

$$\oint \mathbf{E} \cdot \mathbf{dl} = (Z_w I_z - \langle E_z \rangle)\Delta z + \varphi(z+\Delta z) - \varphi(z),$$

$$\text{where} \quad \varphi(z) = \int_{r_0}^{a/2} E_x(x,z)dx. \qquad (4)$$

The electric field circulation equals minus the time derivative of the magnetic flux that penetrates the area bounded by the integration path: $\oint \mathbf{E} \cdot \mathbf{dl} = -j\omega\Phi = -j\omega L I_z \Delta z$, from which we immediately get Eq. (2) when $\Delta z \to 0$.

In general, the effective inductance L depends on the specific microstructure of the system (e.g., if the wires are coated or not with some material). In the particular case in which the wires are conducting cylinders (with no material coating), it was shown,[5] by calculating the magnetic flux of a pair of neighboring wires in the quasistatic approximation, that L is given by

$$L = \frac{\mu_0}{2\pi} \log \frac{a^2}{4r_0(a-r_0)}. \qquad (5)$$

It may be verified that the above formula also applies to the case where the wires are loaded with metallic patches (Fig. 1, right).

The additional potential φ is found by placing a linear charge density ρ on the wires and integrating the corresponding fluctuating part of the microscopic electric field. Thus, ρ is responsible for the electric field component orthogonal to the wires. We introduce an effective capacitance C per unit length, such that it verifies

$$\varphi(z) = \frac{\rho(z)}{C}. \qquad (6)$$

Notice that the considered capacitance is calculated by placing an *identical* linear charge density over the wires (differently from the traditional definition of capacitance, which assumes that charge density over two conductors is antisymmetric). In the same manner as the inductance, the capacitance depends on the microstructure of the system. In the quasistatic limit, a pair of charged wires (with no attached conducting bodies) induces the field (see Fig. 1)

$$E_x = \frac{\rho}{2\pi\varepsilon_0}\left[\frac{1}{x} - \frac{1}{a-x}\right]. \qquad (7)$$

This expression has the same form as the one used in Ref. 5 for the quasistatic magnetic field of a pair of lines of current. Therefore, for this particular case, the capacitance is given by

$$\frac{1}{C} = \frac{1}{2\pi\varepsilon_0} \log \frac{a^2}{4r_0(a-r_0)}. \qquad (8)$$

The capacitance for a system of wires loaded with conducting patches (Fig. 1, right) is calculated in Appendix A.

Considering now a monochromatic plane wave of current excited in the crystal, the currents in the wires can be written in the form

$$I_z(z) = I_0 e^{-jk_z z}, \tag{9}$$

and thus, the linear density of the charge associated with the currents verifies

$$\rho(z) = -\frac{1}{j\omega}\frac{dI_z(z)}{dz} = \frac{k_z}{\omega}I_z(z). \tag{10}$$

Hence, the relation (2) can be rewritten in terms of the effective inductance and of the effective capacitance per unit length of the wire as

$$\langle E_z \rangle = \left(j\omega L + Z_w + \frac{k_z^2}{j\omega C} \right) I_z. \tag{11}$$

Already in this expression, one can identify the spatial dispersion term proportional to the square of the z component of the wave vector.

The macroscopic polarization current in wire media is the average of the currents in separate wires. Let A_{cell} be the average area in the xy plane per one wire of the crystal. Then, the macroscopic polarization current is $J_z = I_z/A_{cell}$. The macroscopic displacement field is $D_z = \varepsilon_0\langle E_z \rangle + J_z/(j\omega)$. Therefore, after some algebra we find that the longitudinal component of the permittivity dyadic is given by

$$\frac{\varepsilon_{zz}}{\varepsilon_0} = 1 - \frac{k_p^2}{k_0^2 - j\xi k_0 - k_z^2/n^2}, \tag{12}$$

where $k_p^2 = \mu_0/(A_{cell}L)$, $n^2 = LC/(\varepsilon_0\mu_0)$, and $\xi = (Z_w/L)\sqrt{\varepsilon_0\mu_0}$. It may be easily checked that the above formula reduces to Eq. (1) in the case of perfectly conducting straight wires ($Z_w = 0$) [also, for unloaded wires $n = 1$ as is seen from Eqs. (5) and (8)]. More generally, when the wires are characterized by the complex permittivity $\varepsilon_0\varepsilon_m$ (e.g., thin plasmonic rods at optical frequencies), the impedance Z_w is given by,

$$Z_w = \frac{1}{j\omega\pi r_0^2\varepsilon_0(\varepsilon_m - 1)}, \tag{13}$$

where r_0 is the radius of the rods. It may be easily verified that in this scenario, Eq. (12) reduces to formula (16) of Ref. 12, which was calculated using a local field based approach. Thus, Eq. (12) generalizes the previous homogenization models of the uniaxial wire medium.

Nevertheless, it is worth noting that the expression for the plasma wavenumber obtained in the present paper differs from the one derived in previous works.[4,12] Namely, under the approach developed above, we have when $A_{cell} \equiv a^2$ (square array)

$$(k_p a)^2 = \frac{2\pi}{\log\dfrac{a^2}{4r_0(a - r_0)}}. \tag{14}$$

In Refs. 4 and 12, under a thin wire approximation, it was obtained that

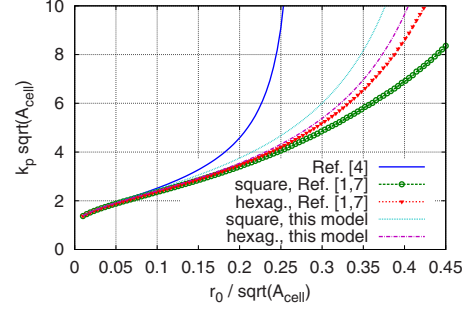$$(k_p a)^2 \approx \frac{2\pi}{0.5275 + \log\dfrac{a}{2\pi r_0}}. \tag{15}$$

FIG. 2. (Color online) The dependence of the normalized plasma frequency $k_p\sqrt{A_{cell}}$ on the normalized wire radius $r_0/\sqrt{A_{cell}}$ for square and hexagonal arrays. For the square array, $A_{cell} = a^2$; for the hexagonal array, $A_{cell} = \sqrt{3}a^2/2$. The lines marked with symbols were calculated using the full wave numerical approaches reported in Refs. 1 and 7, which yielded coincident results.

One can notice that Eq. (15) gives unphysical results for any $r_0/a \geq (2\pi)^{-1}\exp(0.5275) \approx 0.27$. Differently, Eq. (14) gives a qualitatively correct result in the limit $r_0 \to a/2$ when the surfaces of the two wires nearly touch: it predicts an infinite growth in the magnitude of k_p in this limit. It must be noted, however, that in this situation the approximations we use for the magnetic and electric fields of a wire become too rough so that we cannot expect a *quantitatively* correct result in this limit.

For a square array of wires, it can be checked numerically that the accuracy of Eq. (14) is better than that of Eq. (15) when $r_0 \approx 0.1a$ or larger, whereas the opposite behavior is observed for $r_0 < 0.05a$. Nevertheless, both formulas have the same asymptotic behavior when $r_0 \to 0$. At $r_0/a = 0.05$ (this ratio has been used in our numerical simulations that are discussed in Sec. IV), the formulas (14) and (15) overestimate the plasma frequency by about 3%.

This is illustrated in Fig. 2, where the normalized plasma wavenumber is computed using the quasistatic model and two different full wave numerical approaches, for both square and hexagonal lattices.[1,7] It is seen that far from the touching point, the difference in the unit cell geometry has very little impact. It is also seen that the value of the plasma frequency resulting from our quasistatic model is more accurate for the hexagonal lattice. This is expectable as the hexagonal lattice has rotational symmetry of a higher order. Therefore, the field distribution around a wire in such a lattice is more uniform and is better approximated by the simple quasistatic expressions that we use. When $r_0 \lesssim a/5$, the accuracy of our formula is within 10% for both geometries.

Another asymptotic expression for the normalized plasma frequency that is often cited was obtained in Refs. 2 and 3, but even for rather small wire radii its accuracy is worse than that of Eqs. (14) and (15). Also, it does not predict the infinite growth of k_p when $r_0 \to a/2$.

It should be emphasized that Eq. (12) is, in principle, valid for a wide class of wire media (e.g., wires with attached conducting bodies). The parameters C and L depend on the specific microstructure of the system. The magnitude of the spatial dispersion term k_z^2/n^2 in Eq. (12) can be reduced by increasing the value of $n = \sqrt{LC/(\varepsilon_0\mu_0)}$. This quantity has the

meaning of slow-wave factor for quasi-TEM waves propagating along the wires. As mentioned before, for unloaded straight wires $n=1$. As discussed in Ref. [15], the capacitance C can be increased by loading wires with metallic patches and the inductance L can be increased by placing wires in ferromagnetic shields. An alternative way to increase the inductance is to use helices instead of straight wires. Associated bianisotropy in helix medium can be compensated if both right- and left-handed helices are used.

Attaching metallic or dielectric bodies to the wires also changes the transverse components of the permittivity dyadic. We will study this effect with more details in Sec. IV.

III. WIRE MESH

The three-dimensional wire mesh is a wire crystal formed by three mutually orthogonal sets of wires joined at the intersection points. The electromagnetics of such metamaterial have been studied in several recent works.[11,13,19,20] In the following derivation, we assume a cubic lattice, but after a straightforward generalization, the same method can be applied to structures of more complex geometries. Similar to the case studied in Sec. II, metallic or dielectric bodies may be attached to the wires.

In the wire mesh, we get three components of the polarization current related with the currents in three orthogonal sets of wires. The currents in the wires are related to the average electric field in the medium in a manner similar to the uniaxial case

$$\langle E_x \rangle = (j\omega L + Z_w)I_x + \frac{\partial \varphi}{\partial x}, \tag{16}$$

$$\langle E_y \rangle = (j\omega L + Z_w)I_y + \frac{\partial \varphi}{\partial y}, \tag{17}$$

$$\langle E_z \rangle = (j\omega L + Z_w)I_z + \frac{\partial \varphi}{\partial z}. \tag{18}$$

Because the wires are joined at the crossing points, they are locally under the same potential, which is why we have the same φ in all three equations. But the currents in three sets of wires can differ, and that is taken into account by the variables I_x, I_y, and I_z.

Let us consider a unit cell of the wire mesh with three intersecting connected wires. The total charge q accumulated on these three wires per unit cell can be found as

$$q = -\frac{a}{j\omega}\left(\frac{dI_x}{dx} + \frac{dI_y}{dy} + \frac{dI_z}{dz}\right). \tag{19}$$

Because the wires are electrically connected and their effective capacitance per unit length is the same, this charge is equally distributed among the three wires in the unit cell. Therefore, for the linear charge densities on the wires we have in a vicinity of the unit cell

$$\rho_x = \rho_y = \rho_z = \frac{q}{3a} = -\frac{1}{3j\omega}\left(\frac{dI_x}{dx} + \frac{dI_y}{dy} + \frac{dI_z}{dz}\right). \tag{20}$$

Using the same notation for the effective capacitance of a wire as above, we can write the potential φ as

$$\varphi = -\frac{1}{3j\omega C}\left(\frac{dI_x}{dx} + \frac{dI_y}{dy} + \frac{dI_z}{dz}\right) = \frac{1}{3\omega C}(k_x I_x + k_y I_y + k_z I_z), \tag{21}$$

where we have taken into account that the currents on the wires change on average as

$$I_n = I_n^0 e^{-jk_n n}, \quad n = x, y, z. \tag{22}$$

Now, we can substitute this expression for the additional potential into Eqs. (16)–(18). Doing this, we obtain the following system of equations:

$$\langle E_x \rangle = \left(j\omega L + Z_w + \frac{k_x^2}{3j\omega C}\right)I_x + \frac{k_x}{3j\omega C}(k_y I_y + k_z I_z), \tag{23}$$

$$\langle E_y \rangle = \left(j\omega L + Z_w + \frac{k_y^2}{3j\omega C}\right)I_y + \frac{k_y}{3j\omega C}(k_z I_z + k_x I_x), \tag{24}$$

$$\langle E_z \rangle = \left(j\omega L + Z_w + \frac{k_z^2}{3j\omega C}\right)I_z + \frac{k_z}{3j\omega C}(k_x I_x + k_y I_y). \tag{25}$$

By introducing a vector of currents $\mathbf{I} = I_x \mathbf{x}_0 + I_y \mathbf{y}_0 + I_z \mathbf{z}_0$, we rewrite this system in a more compact form using dyadics

$$\langle \mathbf{E} \rangle = \left[(j\omega L + Z_w)\bar{\bar{I}} + \frac{\mathbf{kk}}{3j\omega C}\right] \cdot \mathbf{I}, \tag{26}$$

where $\bar{\bar{I}}$ is the unit dyadic and $\mathbf{kk} \equiv \mathbf{k} \otimes \mathbf{k}$ is the dyadic (tensor) product of two vectors. Now, it is only a matter of inverting the dyadic in brackets of Eq. (26) to get the permittivity dyadic of the wire mesh.

The average polarization in the medium is $\mathbf{P} = \mathbf{I}/(j\omega A_{\text{cell}}) + \mathbf{P}_t$, where $\mathbf{P}_t$ accounts for additional polarization due to finite thickness of the wires or metallic bodies attached to the wires. For a crystal of cubic symmetry, we can write $\mathbf{P}_t = \varepsilon_0(\varepsilon_t - 1)\langle \mathbf{E} \rangle$, where ε_t is the relative transverse permittivity. Therefore, the displacement vector is $\mathbf{D} = \varepsilon_0 \varepsilon_t \langle \mathbf{E} \rangle + \mathbf{I}/(j\omega A_{\text{cell}})$, and

$$\frac{\bar{\bar{\varepsilon}}(\omega, \mathbf{k})}{\varepsilon_0} = \varepsilon_t \bar{\bar{I}} + \frac{1}{j\omega\varepsilon_0 A_{\text{cell}}}\left[(j\omega L + Z_w)\bar{\bar{I}} + \frac{\mathbf{kk}}{3j\omega C}\right]^{-1}, \tag{27}$$

or, after some dyadic algebra,

$$\frac{\bar{\bar{\varepsilon}}(\omega, \mathbf{k})}{\varepsilon_0} = \left(\varepsilon_t - \frac{k_p^2}{k_0^2 - j\xi k_0}\right)\bar{\bar{I}} - \frac{k_p^2 \mathbf{kk}}{3n^2[k_0^2 - j\xi k_0][k_0^2 - j\xi k_0 - k^2/(3n^2)]}, \tag{28}$$

where we use the same notations as in Eq. (12), and $k^2 = k_x^2 + k_y^2 + k_z^2$. The obtained permittivity dyadic can be also rewritten as

$$\frac{\bar{\bar{\varepsilon}}(\omega,\mathbf{k})}{\varepsilon_0} = \varepsilon_{\text{tr}}(\omega)\left(\bar{\bar{I}} - \frac{\mathbf{k}\mathbf{k}}{k^2}\right) + \varepsilon_{\text{lo}}(\omega,k)\frac{\mathbf{k}\mathbf{k}}{k^2}, \qquad (29)$$

where

$$\varepsilon_{\text{tr}}(\omega) = \varepsilon_t - \frac{k_p^2}{k_0^2 - j\xi k_0}, \qquad (30)$$

$$\varepsilon_{\text{lo}}(\omega,k) = \varepsilon_t - \frac{k_p^2}{k_0^2 - j\xi k_0 - k^2/(3n^2)}. \qquad (31)$$

It can be verified that for the mesh of thin plasmonic rods without loading [for which Z_w is given by Eq. (13)], the relations (30) and (31) transform to the ones presented in Ref. 13 with the parameters $\varepsilon_t = 1$ and $k_p = \beta_p$, and identifying the numerical coefficient l_0 from the same reference with $l_0 = 3n^2$.

IV. UNIAXIAL WIRE MEDIUM LOADED WITH PATCHES AND SUPPRESSION OF SPATIAL DISPERSION

Recently,[15] it was proposed to load the wire mesh with metal patches to increase the effective capacitance of the wires per unit length and decrease the related spatial dispersion effects. This proposal was supported by numerical simulations. Here, we will apply our general analytical model to the particular case of a uniaxial wire medium (with the square unit cell) loaded with metal patches. For this purpose, we just need to determine what is the effective capacitance C introduced in Sec. II in the presence of patches. The details of calculation of this capacitance are described in Appendix A. Here, we give the result: $C = C_{\text{wire}} + C_{\text{patch}}$, where C_{wire} is the wire capacitance given by Eq. (8) and

$$C_{\text{patch}} = \frac{2\pi\varepsilon_0 w}{h \log\left(\sec\frac{\pi d}{2a}\right)}, \qquad (32)$$

where w is the width of the square patches periodically attached to the wires and separated by the distance h along z, and $d = a - w$ is the gap between two adjacent patches on a pair of neighboring wires. Thus, the permittivity dyadic of the uniaxial wire medium loaded with patches is given by

$$\frac{\bar{\bar{\varepsilon}}}{\varepsilon_0} = \varepsilon_t \bar{\bar{I}}_t + \left(1 - \frac{k_p^2}{k_0^2 - j\xi k_0 - k_z^2/n^2}\right)\mathbf{z}_0\mathbf{z}_0, \qquad (33)$$

where we keep the same notations as in Sec. II. The transverse permittivity ε_t is mostly determined by the patches when $w \gg r_0$, and it can be found as the permittivity of a stack of capacitive grids separated by h one from another. With the help of the known theory of such grids,[21] it can be found that

$$\varepsilon_t = 1 + \frac{2w}{\pi h}\log\left(\csc\frac{\pi d}{2a}\right). \qquad (34)$$

The accuracy of Eqs. (32) and (34) is better for small gaps and for large values of h/a.

In the limit $d \to 0$, the effective capacitance behaves as $C \approx 16\varepsilon_0 w a^2/(\pi h d^2)$ and, therefore, can be arbitrarily large

if the gap between two adjacent patches is made small enough. On the other hand, the transverse permittivity ε_t grows under the same limit as $\varepsilon_t \approx (2w/\pi h)\log(2a/\pi d)$. The square of the slow-wave factor n^2 is proportional to the effective capacitance, therefore, by increasing the width of the patches one can discard the spatial dispersion term in the right-hand side of Eq. (33) while keeping ε_t at a reasonable level (this is possible because ε_t grows more slowly when $d \to 0$). An explicit expression for the slow-wave factor under the mentioned limit reads

$$n^2 = \frac{LC}{\varepsilon_0\mu_0} \approx 1 + \frac{16w}{\pi h(k_p d)^2}. \qquad (35)$$

In fact, we have numerically checked that this simple expression works quite well for gaps of width $d \lesssim 0.2a$.

To illustrate the suppression of the spatial dispersion in the considered wire media, we have calculated the dispersion diagrams for several configurations using our quasistatic model, the transfer matrix method described in Appendix B, and the eigenmode solver of CST Microwave Studio. The structure was assumed lossless in the simulations (all metallic components are perfectly conducting so that $Z_w = 0$). The transfer matrix formalism developed in Appendix B is based on the assumption that in between two patch grids the electric field is a superposition of TEM and TM modes.[9] The fields on the interfaces of each patch grid are linked by a grid impedance and by an additional boundary condition,[22] consistent with the formalism described in Refs. 16 and 17. The obtained results are presented in Fig. 3.

In Figs. 3(a) and 3(c) the dispersion diagrams obtained from the quasistatic model and the numerical simulations are shown for a set of the propagation angles with respect to the axis of the structure: $\alpha = 0, 30°, 60°$ [for the other parameters of the structure refer to Fig. 1; in these plots the wave vector is $\mathbf{k} = k(\sin\alpha\mathbf{x}_0 + \cos\alpha\mathbf{z}_0)$]. The dispersion curves predicted by the quasistatic model are depicted with solid lines while the results of the numerical simulations are represented by symbols. In the example of Fig. 3(a), the patch width has been set equal to $w = 0.5a$, while in Fig. 3(c) the patch width is $w = 0.9a$. In both cases the theory and the simulations predict the existence of two dispersion branches associated with extraordinary waves, i.e., with the quasi-TEM and TM modes, as well as a dispersion branch associated with the ordinary (TE) wave whose dispersion is not depicted in Fig. 3 (there are also other higher order modes at higher frequencies, but we are not interested in them). We call the high-frequency branch "the plasmon mode" because for $\alpha = 0$ this branch corresponds to the longitudinal plasmon-type wave propagating along the axis of the structure. On the other hand, the low-frequency branch for $\alpha = 0$ belongs to an ordinary transverse wave, which is not affected by the wires (but it is affected by the transverse permittivity ε_t of the medium).

From Fig. 3(a), one can see that for the moderate-size patches the quasistatic model works surprisingly well even when ka approaches π. The small difference in the frequencies of the plasmon-type modes predicted by the theory and the simulations at $ka = 0$ is due to the asymptotic nature of the formula for the plasma wavenumber that we use (the discussion on this is given in Sec. II). For larger patches [Fig.
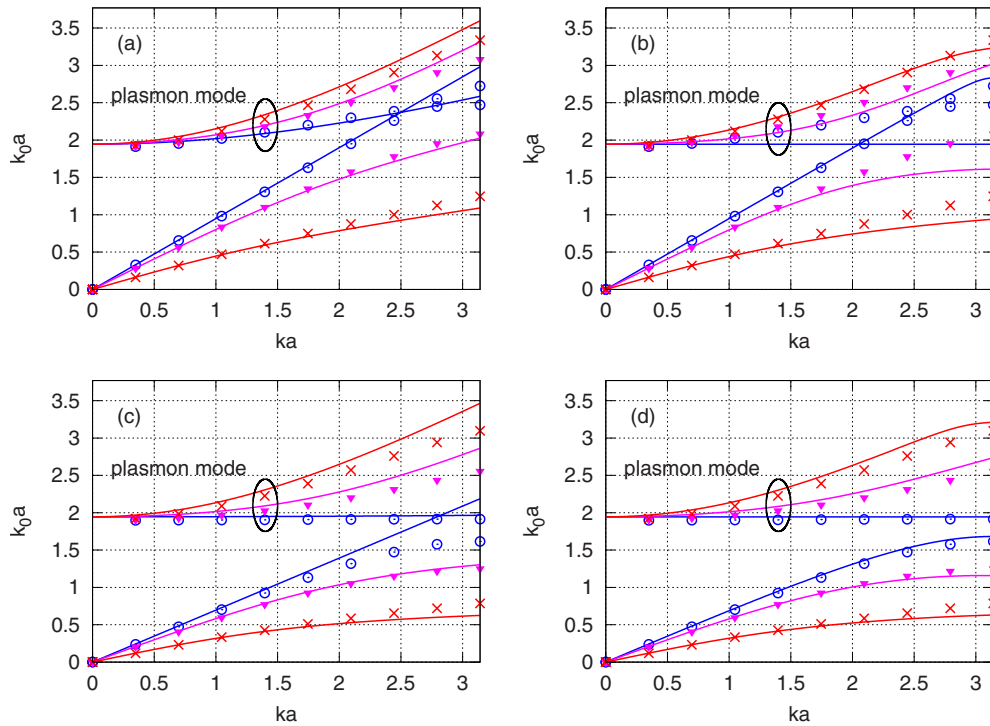
FIG. 3. (Color online) Dispersion diagrams for a uniaxial wire medium loaded with patches obtained using two analytical models and numerical simulations for different propagation angles α with respect to the z axis. Only the branches associated with the quasi-TEM and TM modes are shown. Panels (a) and (c): quasistatic model vs numerical simulations: (a) $w=0.5a$ and (c) $w=0.9a$. Panels (b) and (d): transfer matrix model vs numerical simulations: (b) $w=0.5a$ and (d) $w=0.9a$. On all four panels, the solid lines represent the analytical results and the symbols correspond to the results of numerical simulations; the values of the propagation angles are coded in color: $\alpha=0$: blue lines and circles; $\alpha=30°$: magenta lines and triangles; $\alpha=60°$: red lines and crosses. The other parameters in all four cases: $r_0=0.05a$ and $h=a$.

3(c)], the quasistatic model does not predict appearance of a band gap at $\alpha=0$ and $ka=\pi$. This is expected since in the model the capacitive loading on the wires is assumed to be effectively uniform along the wires.

Figures 3(b) and 3(d) display the same dispersion diagrams but with the quasistatic model replaced by the transfer matrix model described in Appendix B. One can see that this model wrongly predicts a completely flat dispersion for the plasmon mode propagating along the z axis ($\alpha=0$), independently of the patch size. This is in disagreement with the numerical simulations, as is seen from Fig. 3(b). Indeed, the formalism developed in Refs. 16 and 17 is only valid when the gap between the patches is small, because otherwise other higher modes can be excited near the connections of the wires to the patch grid, and in such conditions it is not possible to consider that the microscopic field in the vicinity of the connection points are a superposition of TM and TEM modes of the unloaded wire medium, as assumed in Refs. 16 and 17. Consistent with this observation, it is seen in Fig. 3(d), that for larger patches and (or) larger angles of propagation the disagreement is less pronounced. Another characteristic feature of the transfer matrix model is that it is able to predict the existence of the above-mentioned bandgap. This is because the transfer matrix model takes into account the granularity of the structure along the z axis.

The suppression of the spatial dispersion effects is evident if we compare Fig. 3(a) with Fig. 3(c). Indeed, the latter case corresponds to a larger patch width ($w=0.9a$), and conse-

quently, the slope of the dispersion curve associated with the longitudinal mode (the plasmon mode at $\alpha=0$) is very small. To justify this effect and also to check the accuracy of the quasistatic model near the origin of the Brillouin zone for a wide range of values of the gap, we have extracted the values of the slow wave factor n from the results of the numerical simulations slightly above the point $ka=0$ and compared them with the value of n given by the analytical model. The results of this extraction are presented in Fig. 4. From this figure, we see that despite its simplicity, the quasistatic
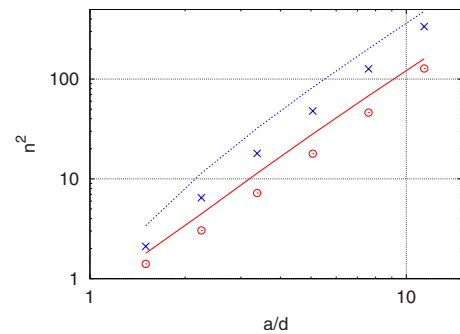

FIG. 4. (Color online) The square of the slow-wave factor as a function of a/d (logarithmic scale). The lines represent the result of the quasistatic model, the symbols correspond to the values of n^2 extracted from the numerical simulations. Blue dotted line and crosses: $r_0=0.05a$ and $h=a/3$; red solid line and circles: $r_0=0.05a$ and $h=a$.

model predicts very well the trend in the growth of n^2 when the gap between the patches decreases. The agreement tends to improve for larger values of h/a.

V. CONCLUSIONS

In this paper, we have developed a quasistatic analytical model of wire media applicable to a wide class of structures, and in particular we have considered uniaxial and isotropic wire crystals, which may be loaded with metallic patches. Because the developed model is defined in simple physical terms of the effective inductance and capacitance per unit length of a wire, it can be readily extended to other wire structures of more complex geometries. The model accounts for the finite conductivity of the wires so that it can be applied in case of plasmonic effects (consistent with the results reported in Refs. [12] and [13]) or when the wires are uniformly loaded with arbitrary complex impedances. In particular, we have studied with details the electrodynamics of uniaxial wire media loaded with patches, and demonstrated with full wave simulations that the proposed quasistatic model describes accurately the properties of the system in the long wavelength limit. Consistent with the analysis of Refs. [15]–[17], it was shown that the presence of the patches may result in a dramatic reduction in the nonlocal effects. For the case of unloaded wire media, we have demonstrated that the quasistatic model yields the same expressions for the dielectric permittivity tensors as those obtained by much more sophisticated methods.[6,8,10–13] Thus, we have proven that the strong spatial dispersion in wire media is a quasistatic effect. Although this fact has already been noticed,[14] the presented research extends the results obtained in Ref. [14] and allows for analytical and quantitative studies of the possibilities to control the spatial dispersion in wire media.

APPENDIX A

As is seen from Fig. 1 (right) that depicts the path along which we calculate the circulation of the electric field, the capacitance in question can be calculated if we find the electric field in the region close to the gap between two patches on the neighboring wires. Indeed, the circulation integral (3) in the presence of patches has to be modified as follows:

$$\oint \mathbf{E} \cdot \mathbf{dl} = \int_{z_0}^{z_0+h} E_z(r_0,z)dz - \int_{z_0}^{z_0+h} E_z(a/2,z)dz$$
$$+ \int_{w/2}^{a/2} E_x(x,z_0+h)dx - \int_{w/2}^{a/2} E_x(x,z_0)dx,$$
$$\text{(A1)}$$

where z_0 is at the location of an arbitrary plane of patches. We choose the integration path so that it first goes along the

surfaces of the wire and the patch till the gap, then across the gap till the symmetry line (Fig. 1), then along that line until the second gap and then across this gap back to the patch and the wire.

One can see that the first integral in the right-hand side of Eq. (A1) still represents the same quantity as in the unloaded uniaxial wire medium and is related to the finite conductivity of the wire. The integrals along the surfaces of the patches are not shown in Eq. (A1) as in the following we consider the patches to be ideally conducting. This may be a good approximation, because, in practice, the wire impedance dominates. We can express the second integral of Eq. (A1) as

$$\int_{z_0}^{z_0+h} E_z(a/2,z)dz = \langle E_z \rangle h - \varphi_z(z_0 + h) + \varphi_z(z_0), \quad \text{(A2)}$$

where the two last terms account for the strong nonuniformity of the z component of the microscopic electric field in the vicinity of the gaps and can be defined (in the unit cell $z_0 \leq z \leq z_0+h$) as

$$\varphi_z(z) = \int_z^{z_0+h/2} [E_z(a/2,z) - \langle E_z \rangle]dz. \quad \text{(A3)}$$

Notice that when there are no patches the microscopic field changes smoothly along z; that is why in Sec. II, we could simply relate the second integral of Eq. (A1) with the macroscopic electric field. The two remaining integrals can be written in terms of

$$\varphi_x(z) = \int_{w/2}^{a/2} E_x(x,z)dx. \quad \text{(A4)}$$

Substituting the above expressions for the integrals into Eq. (A1) and comparing it with Eq. (4) with $\Delta z = h$, we see that the additional potential at the plane $z = z_0$ has to be

$$\varphi(z_0) = \varphi_x(z_0) + \varphi_z(z_0). \quad \text{(A5)}$$

At this point, it is worth reminding that the additional potential as we define it and use it in Secs. II and III is essentially a macroscopic quantity: it changes slowly and smoothly along the wires. Therefore, Eq. (A5) can be understood as the definition of the averaging procedure for the additional electric field (represented by both nonuniform E_x and E_z components) that appears because of the periodical nonuniformity in the charge distribution introduced by the patches.

It is clear that for wide patches, this additional potential is mainly determined by the fluctuating part of the microscopic field in the vicinity of the gap at $x = a/2$, $z = z_0$. Thus, to simplify the problem we may first neglect the effect of the charges sitting on the wires (nevertheless, we will later add a correction term taking the wires into account). Second, because $\varphi(z_0)$ depends only on the nonuniform part of the field we may neglect the effect of all other planes of charged patches except the plane $z = z_0$. We may do so, because when $h \gg d = a - w$, the field produced by the other planes of patches is practically uniform in the vicinity of the gap we are interested in. Therefore, in the following, we consider only a single array of charged patches and discard all the patches that are not co-planar with the patch at $z = z_0$.
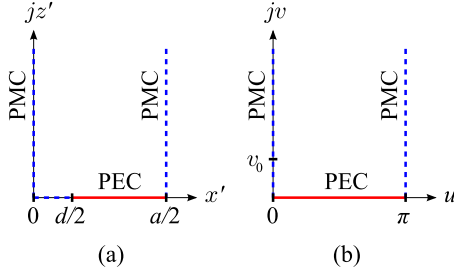
FIG. 5. (Color online) The original domain (a) and the domain obtained after the conformal mapping (b) defined by Eq. (A6). The solid red lines represent the perfect electric conductor boundary (PEC) (surface of the patch), and the dashed blue lines represent the perfect magnetic conductor (PMC) boundaries that impose necessary symmetries. The point v_0 corresponds to the origin of the domain (a).

In what follows, we will solve the enunciated electrostatic problem and calculate the effective capacitance per unit length of a wire with patches. In order to obtain a closed-form analytical solution, we will make an additional simplification: we replace all the patches centered at the same y coordinate with a single metal strip of the same width. Thus, we obtain a grid of metallic strips (geometry of the problem becomes invariant along y) separated by the same gap as the array of patches.

Taking into account the symmetry of the excitation and the periodicity of the grid we arrive at the two-dimensional problem shown in Fig. 5(a). In this figure, we define the local coordinate system x', z' as follows. The middle point of the gap is at $x' = z' = 0$. The patch is modeled as an infinitely thin perfect electric conductor (PEC) strip, which starts at $x' = d/2$ and continues to the point $x' = a/2$, which is at the middle line of the patch. The strip is charged. The perfect magnetic conductor (PMC) boundaries shown in the figure enforce the symmetries mentioned above.

The distribution of the electric potential in this system can be found with the conformal mapping approach.[23] One can verify that the following analytical function of the complex variable $\mathcal{Z} = x' + jz'$:

$$\zeta(\mathcal{Z}) = u(x', z') + jv(x', z')$$

$$= \cos^{-1}\left[\frac{2\cos\dfrac{2\pi\mathcal{Z}}{a} - \cos\dfrac{\pi d}{a} + 1}{\cos\dfrac{\pi d}{a} + 1}\right] \quad \text{(A6)}$$

maps the domain shown in Fig. 5(a) into the domain of Fig. 5(b) in which the solution for the electric field is trivial. One can see that the curves $v(x', z') = \text{const}$ are the equipotential contours and the curves $u(x', z') = \text{const}$ are the force lines of the electric field of the problem. It can be checked that at the patch, the potential defined in this way vanishes: $v(x', 0) = 0$ for $d/2 \le x' \le a/2$.

Therefore, the voltage drop between a distant point on the z' axis (which is a point on the integration path shown in Fig. 1) and the edge of the patch is

$$v(0, z') = \cosh^{-1}\left[\frac{2\cosh\dfrac{2\pi z'}{a} - \cos\dfrac{\pi d}{a} + 1}{1 + \cos\dfrac{\pi d}{a}}\right]. \quad \text{(A7)}$$

When $z' \gg d$, this voltage asymptotically behaves as

$$v(0, z') \sim 2\log\left(\sec\frac{\pi d}{2a}\right) + \frac{2\pi z'}{a}. \quad \text{(A8)}$$

The linearly growing term of Eq. (A8) corresponds to a uniform electric field far away from the gap. Such a smooth field is already taken into account by the first term of Eq. (A2). Therefore, the additional potential we are looking for must be defined as

$$\varphi(z_0) = \lim_{z' \to \infty}\left(v(0, z') - \frac{2\pi z'}{a}\right) = 2\log\left(\sec\frac{\pi d}{2a}\right). \quad \text{(A9)}$$

On the other hand, the total charge per unit length of the strip is given by

$$Q = 4\varepsilon_0[u(a/2, 0) - u(d/2, 0)] = 4\pi\varepsilon_0, \quad \text{(A10)}$$

where the coefficient 4 accounts for the fact that the domain of Fig. 5(a) includes only 1/4 of the total surface of the strip. Hence, the effective capacitance per unit length of a strip is $C_{\text{strip}} = Q/\varphi(z_0)$ and the effective patch capacitance per unit length of a wire with patches is $C_{\text{patch}} = (w/h)C_{\text{strip}}$, which is given by Eq. (32). The total capacitance per unit length of a wire with patches is approximated as a sum of the wire capacitance C_{wire} from Eq. (8) and C_{patch}.

APPENDIX B

The uniaxial wire medium periodically loaded with patches may be regarded as a layered structure. Thus, it is possible to apply the standard transfer matrix method to it, provided we are able to characterize the fields in one cell. As demonstrated next, this can be done by generalizing the formalism developed in Refs. 16 and 17, which is based on the assumption that in the regions in between two arbitrary adjacent patch grids the microscopic fields can be written as a superposition of TM and TEM modes of the unloaded wire medium.

Suppose that the wires are directed along z and that the magnetic field is along the y direction (the TM polarization). The electric field components are E_x and E_z and the wave vector is $\mathbf{k} = k_x \mathbf{x}_0 + k_z \mathbf{z}_0$. The fields in the region $0 < z < h$ ($z = 0$ at the patch array) in between two arrays of metallic patches can be decomposed into four waves

$$\eta_0 H_y = A_{\text{TM}}^+ e^{-\gamma_{\text{TM}}z} + A_{\text{TM}}^- e^{+\gamma_{\text{TM}}z} + B_{\text{TEM}}^+ e^{-\gamma_{\text{TEM}}z} + B_{\text{TEM}}^- e^{+\gamma_{\text{TEM}}z}, \quad \text{(B1)}$$

$$E_x = \frac{j}{\varepsilon_h k_0}\frac{d}{dz}(\eta_0 H_y) = -\frac{j}{\varepsilon_h k_0}[\gamma_{\text{TM}}(A_{\text{TM}}^+ e^{-\gamma_{\text{TM}}z} - A_{\text{TM}}^- e^{+\gamma_{\text{TM}}z})$$
$$+ \gamma_{\text{TEM}}(B_{\text{TEM}}^+ e^{-\gamma_{\text{TEM}}z} + B_{\text{TEM}}^- e^{+\gamma_{\text{TEM}}z})], \quad \text{(B2)}$$

$$E_z = \frac{-k_x}{\varepsilon_{zz}^{\mathrm{TM}} k_0}(A_{\mathrm{TM}}^+ e^{-\gamma_{\mathrm{TM}} z} + A_{\mathrm{TM}}^- e^{+\gamma_{\mathrm{TM}} z}), \qquad (B3)$$

where ε_h is the permittivity of the host material relative to the free space permittivity, $\gamma_{\mathrm{TM}} = \sqrt{k_p^2 + k_x^2 - \varepsilon_h k_0^2}$, $\gamma_{\mathrm{TEM}} = j\sqrt{\varepsilon_h} k_0$, and $\varepsilon_{zz}^{\mathrm{TM}} = \varepsilon_h k_x^2/(k_p^2 + k_x^2)$. It may be easily recognized that the above expressions correspond to a superposition of the standard TEM and TM modes supported by the unloaded wire medium.[9]

The tangential components of the fields at the planes $z = h^-$ and $z = h^+$ are linked by the transfer matrix of the patch array

$$\begin{pmatrix} E_x \\ \eta_0 H_y \end{pmatrix}_{z=h^+} = \begin{pmatrix} 1 & 0 \\ -y_{\mathrm{g}} & 1 \end{pmatrix} \cdot \begin{pmatrix} E_x \\ \eta_0 H_y \end{pmatrix}_{z=h^-}, \qquad (B4)$$

where $y_{\mathrm{g}} = (2j\varepsilon_h k_0 a/\pi)\log[\csc(\pi d/2a)]$ is the normalized effective admittance of the patch array.[16,17] On the other hand, it was shown in Ref. 22 that since the microscopic surface charge density must vanish at the connections between the wires and the grid, the following additional boundary condition (ABC) must be verified

$$k_0 \varepsilon_h \frac{dE_z}{dz} + k_x \eta_0 \frac{dH_y}{dz} = 0, \quad z = 0^+, \quad z = h^-, \qquad (B5)$$

where η_0 is the free-space impedance. Using this ABC in Eqs. (B1)–(B3), it is possible to obtain the coefficients associated with the TEM wave ($B_{TEM}^{\pm}$) as a function of the coefficients associated with the TM wave ($A_{TM}^{\pm}$). Then, $A_{TM}^{\pm}$ can be expressed in terms of the tangential electric and magnetic fields at the $z=0^+$ plane. Proceeding in this manner, it is possible to obtain after lengthy but straightforward calculations the following transfer matrix relation for the layer of the wire medium in between two patch grids

$$\begin{pmatrix} E_x \\ \eta_0 H_y \end{pmatrix}_{z=h^-} = \mathbf{M} \cdot \begin{pmatrix} E_x \\ \eta_0 H_y \end{pmatrix}_{z=0^+}, \qquad (B6)$$

where the matrix $\mathbf{M}$ is

$$\mathbf{M} = \begin{pmatrix} m_{11} & m_{12} \\ m_{21} & m_{11} \end{pmatrix}, \qquad (B7)$$

with the elements given by the following formulas:

$$m_{11} = \frac{(\varepsilon_h - \varepsilon_{zz}^{\mathrm{TM}})\gamma_{\mathrm{TM}}\sinh(\gamma_{\mathrm{TM}}h)\cosh(\gamma_{\mathrm{TEM}}h) + \varepsilon_{zz}^{\mathrm{TM}}\gamma_{\mathrm{TEM}}\cosh(\gamma_{\mathrm{TM}}h)\sinh(\gamma_{\mathrm{TEM}}h)}{(\varepsilon_h - \varepsilon_{zz}^{\mathrm{TM}})\gamma_{\mathrm{TM}}\sinh(\gamma_{\mathrm{TM}}h) + \varepsilon_{zz}^{\mathrm{TM}}\gamma_{\mathrm{TEM}}\sinh(\gamma_{\mathrm{TEM}}h)}, \qquad (B8)$$

$$m_{12} = \frac{1}{k_0}\frac{j\gamma_{\mathrm{TEM}}\gamma_{\mathrm{TM}}\sinh(\gamma_{\mathrm{TM}}h)\sinh(\gamma_{\mathrm{TEM}}h)}{(\varepsilon_h - \varepsilon_{zz}^{\mathrm{TM}})\gamma_{\mathrm{TM}}\sinh(\gamma_{\mathrm{TM}}h) + \varepsilon_{zz}^{\mathrm{TM}}\gamma_{\mathrm{TEM}}\sinh(\gamma_{\mathrm{TEM}}h)}, \qquad (B9)$$

$$m_{21} = -jk_0\left[\frac{2(\varepsilon_h - \varepsilon_{zz}^{\mathrm{TM}})\varepsilon_{zz}^{\mathrm{TM}}[-1 + \cosh(\gamma_{\mathrm{TM}}h)\cosh(\gamma_{\mathrm{TEM}}h)]}{(\varepsilon_h - \varepsilon_{zz}^{\mathrm{TM}})\gamma_{\mathrm{TM}}\sinh(\gamma_{\mathrm{TM}}h) + \varepsilon_{zz}^{\mathrm{TM}}\gamma_{\mathrm{TEM}}\sinh(\gamma_{\mathrm{TEM}}h)} + \frac{\sinh(\gamma_{\mathrm{TEM}}h)\sinh(\gamma_{\mathrm{TM}}h)\left[(\varepsilon_h - \varepsilon_{zz}^{\mathrm{TM}})^2\frac{\gamma_{\mathrm{TM}}}{\gamma_{\mathrm{TEM}}} + (\varepsilon_{zz}^{\mathrm{TM}})^2\frac{\gamma_{\mathrm{TEM}}}{\gamma_{\mathrm{TM}}}\right]}{(\varepsilon_h - \varepsilon_{zz}^{\mathrm{TM}})\gamma_{\mathrm{TM}}\sinh(\gamma_{\mathrm{TM}}h) + \varepsilon_{zz}^{\mathrm{TM}}\gamma_{\mathrm{TEM}}\sinh(\gamma_{\mathrm{TEM}}h)}\right]. \qquad (B10)$$

It may be verified that $\det(\mathbf{M}) = 1$. From Eqs. (B6) and (B4), it is clear that the global transfer matrix of the system is

$$\mathbf{M}_{\mathrm{g}} = \begin{pmatrix} 1 & 0 \\ -y_{\mathrm{g}} & 1 \end{pmatrix} \cdot \mathbf{M}. \qquad (B11)$$

As is well-known, the dispersion characteristic of the Bloch-Floquet modes supported by the periodic structure verifies $\cos(k_z h) = \mathrm{tr}(\mathbf{M}_{\mathrm{g}})/2$, where $\mathrm{tr}(\ldots)$ represents the trace of the matrix. Thus, it follows that dispersion equation for the Bloch-Floquet modes is

$$\cos(k_z h) = m_{11} - \frac{y_{\mathrm{g}}}{2} m_{12}. \qquad (B12)$$

The transfer matrix dispersion diagrams calculated in Sec. IV were obtained using the above equation.

---

*stas@co.it.pt

[1] N. A. Nicorovici, R. C. McPhedran, and L. C. Botten, Phys. Rev. E **52**, 1135 (1995).

[2] J. B. Pendry, A. J. Holden, W. J. Stewart, and I. Youngs, Phys. Rev. Lett. **76**, 4773 (1996).

[3] J. B. Pendry, A. J. Holden, D. J. Robbins, and W. J. Stewart, J. Phys.: Condens. Matter **10**, 4785 (1998).

[4] P. A. Belov, S. A. Tretyakov, and A. Viitanen, J. Electromagn. Waves Appl. **16**, 1153 (2002).

[5] S. I. Maslovski, S. A. Tretyakov, and P. A. Belov, Microwave

Opt. Technol. Lett. **35**, 47 (2002).

[6] A. L. Pokrovsky and A. L. Efros, Phys. Rev. B **65**, 045110 (2002).

[7] M. Silveirinha and C. A. Fernandes, IEEE Trans. Microwave Theory Tech. **51**, 1460 (2003).

[8] G. Shvets, A. K. Sarychev, and V. M. Shalaev, Proc. SPIE **5218**, 156 (2003).

[9] P. A. Belov, R. Marques, S. I. Maslovski, I. S. Nefedov, M. Silveirinha, C. R. Simovski, and S. A. Tretyakov, Phys. Rev. B **67**, 113103 (2003).

[10] C. R. Simovski and P. A. Belov, Phys. Rev. E **70**, 046616 (2004).

[11] M. G. Silveirinha and C. A. Fernandes, IEEE Trans. Microwave Theory Tech. **53**, 1418 (2005).

[12] M. G. Silveirinha, Phys. Rev. E **73**, 046612 (2006).

[13] M. G. Silveirinha, Phys. Rev. B **79**, 035118 (2009).

[14] S. I. Maslovski, Ph.D. thesis, St. Petersburg State Polytechnical University, 2004.

[15] A. Demetriadou and J. B. Pendry, J. Phys.: Condens. Matter **20**, 295222 (2008).

[16] A. B. Yakovlev, M. G. Silveirinha, O. Luukkonen, C. R. Simovski, I. S. Nefedov, and S. A. Tretyakov, IEEE Trans. Microwave Theory Tech. **57**, 2700 (2009).

[17] O. Luukkonen, M. Silveirinha, A. Yakovlev, C. Simovski, I. Nefedov, and S. Tretyakov, IEEE Trans. Microwave Theory Tech. **57**, 2692 (2009).

[18] D. Sievenpiper, L. Zhang, R. Broas, N. Alexopolous, and E. Yablonovitch, IEEE Trans. Microwave Theory Tech. **47**, 2059 (1999).

[19] M. Hudlicka, J. Machác, and I. S. Nefedov, Prog. Electromagn. Res. **PIER 65**, 233 (2006).

[20] M. A. Shapiro, G. Shvets, J. R. Sirigiri, and R. J. Temkin, Opt. Lett. **31**, 2051 (2006).

[21] S. A. Tretyakov, *Analytical Modelling in Applied Electromagnetics* (Artech House, Norwood, MA, 2003).

[22] M. G. Silveirinha, C. A. Fernandes, and J. R. Costa, New J. Phys. **10**, 053011 (2008).

[23] R. Collin, *Field Theory of Guided Waves* (IEEE Press, Piscataway, NJ, 1990).